Black Phosphorus Avalanche Photodetector

Mahmoud R. M. Atalla and Steven J. Koester*

ECE Department, University of Minnesota-Twin Cities, 200 Union St. SE, Minneapolis, MN 55455

**Ph: (612) 625-1316, FAX: (612) 625-4583, Email: skoester@umn.edu*

Introduction: The strong light-matter interaction of atomically-thin layered black phosphorus (BP) has attracted great attention recently. Exfoliated few-layer and monolayer BP flakes have a layer-tunable direct bandgap that varies from 2.0 eV for monolayer to 0.3 eV for bulk, which makes BP a very promising optoelectronic material in the visible and telecom wavelengths [1-3]. The high mobility of BP devices suggested its utilization as an active material of an avalanche photodetector (APD). Recently, APDs utilizing two-dimensional (2D) materials such as transition-metal dichalcogenides (e.g. MoS_2) and layered III-VI semiconductors (e.g. InSe) have been demonstrated [4,5]. Both of these 2D materials possess wide bandgaps that discourage their usage in the infrared [6,7]. The successful demonstration of waveguide-integrated BP photodetector working at 1.55 μm wavelength [1] has stimulated the pursuit of high-performance BP APDs. In this work, we report on the first 2D material-based BP APD featuring high external quantum efficiency (EQE) and avalanche gain. These results provide strong evidence that BP is a promising material for high-performance optical communication and imaging systems.

Device fabrication: The BP APD fabrication started using a Si/SiO_2 substrate on which 7 nm of HfO_2 was deposited at 300 °C using atomic layer deposition (ALD). Exfoliated BP flakes with thicknesses between 7 and 14 nm were then transferred onto the substrate. Finally, Ti (10nm)/ Au (50 nm) contacts were patterned and lifted-off, followed by deposition of Al_2O_3 (20 nm) using ALD at 300 °C. Devices were characterized after the final ALD passivation. The fabrication process flow is shown in Fig. 1. The precise area of the APDs was determined by the shape of the flake, but the typical device size was roughly 10 x 10 μm^2. No attempt was made to control the crystal orientation of the BP flake.

Results and analysis: All measurements were performed in ambient atmosphere at room temperature. The current-voltage curves of the BP APDs in Fig. 2 depict high gain as the optical power and bias increase. Optical mapping measurements were performed using a focused laser beam of wavelength 532 nm, spot size 2 μm^2 and power intensity of 2 $\mu W/\mu m^2$. In Fig. 3, the optical mapping images show the APD current as a function of its *x*- and *y*-coordinates and these results clearly indicate significant electron-hole pair photogeneration that increases as the applied bias increases. Additionally, we observe from Fig. 3 that the photocurrent maps indicate a high photocurrent region near the positive contact at low bias, but this region shifts toward the negative contact as the bias increases. This holds true for both forward and reverse biases. The origin of the photocurrent gain is investigated in Fig. 4. The multiplication factor (M) was computed as the ratio of total current and the pre-multiplication current [8]. According to the APD theory, the dependence of M on the applied bias (V) was found to conform to the empirical law [5,9], $M = 1/(1-(V/V_b)^n)$, where the breakdown voltage V_b and the constant parameter n were determined as shown in Figs. 4(a) and 4(b). Three regions as function of the bias could be distinguished. Region I is the pre-multiplication region, region II is where typical multiplication occurs, and region III is the breakdown region where significant hole tunneling takes place across the Schottky barrier at the contacts as schematically shown in Fig. 4(d). Fig. 4(c) indicates that the avalanche gain reaches 272 at bias 50 V and optical power 19.1 μW. In Fig. 5 a TCAD simulation was implemented to explain the photocurrent origin shift demonstrated in Fig. 3. Figs. 5(a) and 5(b) show the impact-ionization rate using pre-assumed ionization coefficients, tunneling at the contacts and constant photogeneration rate at 10 V and 30 V, respectively. The impact ionization is found to be high in the region near the positive contact at low bias (Region II), but shifts towards the negative contact as the bias increases (Region III), in agreement with experiment. This behavior arises as the hole tunneling significantly increases with voltage. Figs. 6(a) and 6(b) show the calculated absorption in the different layers of the BP APD structure along with the EQE and internal quantum efficiency (IQE) as a function of the gain. Finally, Table 1 presents metrics for the BP APD and comparison with previously reported 2D material-based APDs, which depicts the high gain and EQE of the BP APD. Future improvements for the BP APD design shall be made to get higher gain at lower voltage and reduce the dark current.

Acknowledgement: The work was supported by the AFOSR under grant FA9550-14-1-0277 and the NSF under grant ECCS-1648782. Portions of this work were carried out in the UMN Characterization Facility which receives support from NSF through the MRSEC program under Award DMR-1420013.

[1] N. Youngblood, *et al*., *Nat. Photon.*, 2015; [2] S. Das, *et al, Nano Lett.,* 2014; [3] Y. Takao, *et al., J. Phys. Soc. Jpn.,* 1981; [4] O. Lopez-Sanchez, *et al*., *arXiv*, 2014; [5] S. Lei, *et al*., *Nano Lett.,* 2015; [6] Q. H. Wang, *et al., Nat. Nanotech.*, 2012; [7] O. Lopez-Sanchez, *et al.*, *Nat. Naonotech.,* 2013; [8] M. H. Woods, *et al., Solid-State Electron.,* 1973; [9] S. L. Miller, *Phys. Rev.,* 1957.

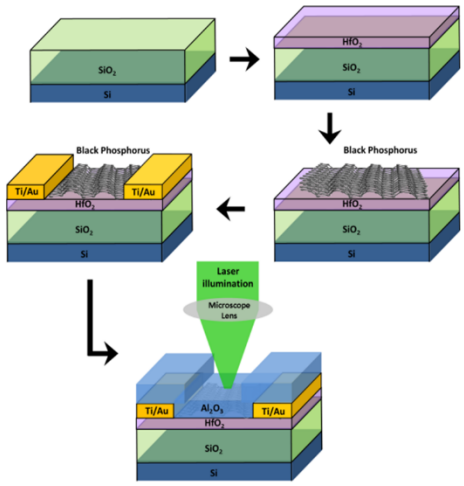

Fig. 1. Fabrication sequence for BP APDs.

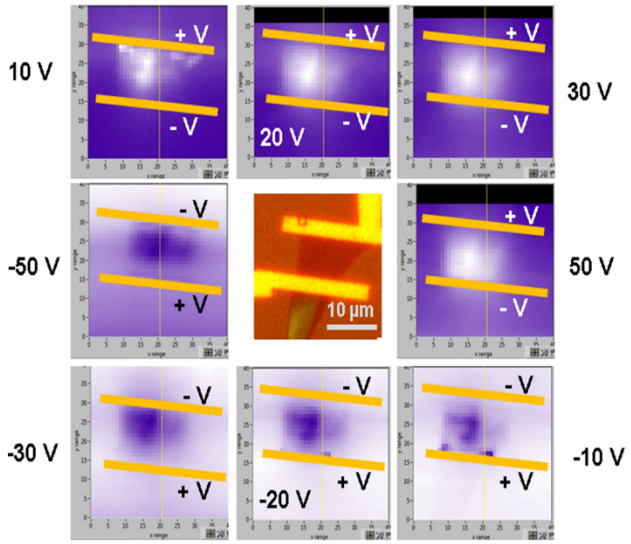

Fig. 3. Optical mapping of BP APD. A focused green laser beam with 2 μm^2 spot size was utilized to map the photocurrent of the APD. In the center is an optical micrograph of the BP APD and it is surrounded by optical mapping graphs collected at the prescribed biases and at the same optical power 2 μW/μm^2. A shift in the photocurrent origin as the bias increases is evident.

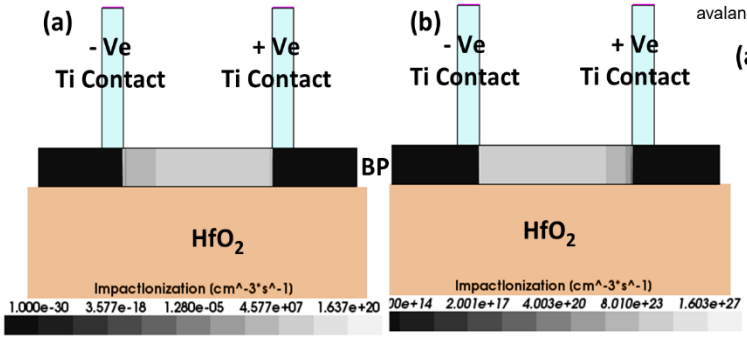

Fig. 5. Simulation of impact ionization generation rate under green light illumination inside the APD at biases: (a) 10 V and (b) 30 V. The shift in the photocurrent origin as the bias increases is due to significant hole tunneling through the Schottky barrier at the contacts.

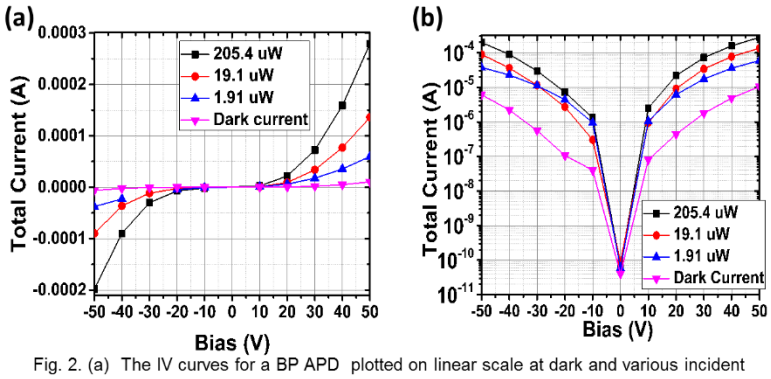

Fig. 2. (a) The IV curves for a BP APD plotted on linear scale at dark and various incident optical powers. (b) the same as (a) except that the current is displayed on logarithmic scale.

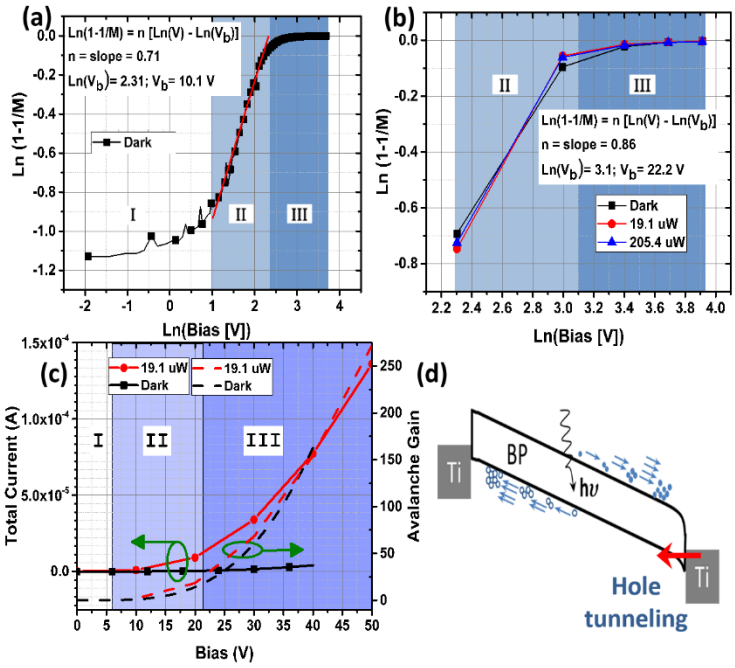

Fig. 4. (a) The dark current of one of the APDs conforming with the prescribed empirical law with M, V, and V_b are the multiplication factor, applied bias, breakdown voltage, respectively. This plot depicts no multiplication in region I, avalanche multiplication region II and breakdown region III, respectively. (b) is same as (a) but for another APD. (c) The total current and avalanche gain versus bias for the same device in (b). (d) Band diagram illustrates the avalanching and the tunneling inside the APD.

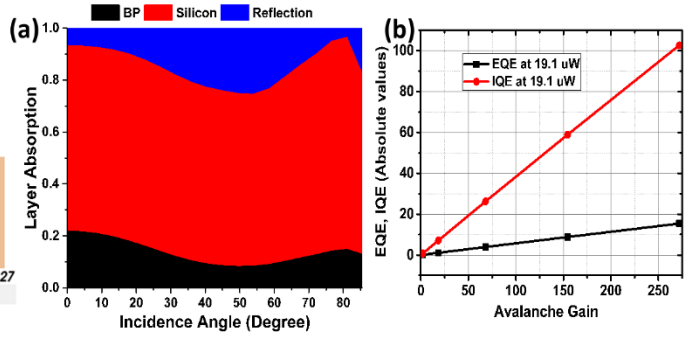

Fig. 6. (a) layer absorption of the BP APD as function of incidence angle and (b) presents the EQE and IQE of the APD as function of avalanche gain.

	BP APD (This work)	InSe APD (Ref. 5)	MoS_2 /Si APD (Ref. 4)
Gain	272 at E_{eff} = 5 x 10^6 V/m	152 at E_{eff} = 35 x 10^6 V/m	1000 at E_{eff} = 9 x 10^6 V/m
EQE*	2.719 at gain = 47	3.44 at gain = 47	0.9794** at gain = 1000
IQE*	18.125 at gain = 47	----	9.794** at gain = 1000
Dark current	10.5 μA at E_{eff} = 5 x 10^6 V/m	1.3 nA at E_{eff} = 35 x 10^6 V/m	0.2 μA at E_{eff} = 9 x 10^6 V/m

Table 1. Performance metrics for BP APDs described in this work compared with 2D material-based InSe APD reported in [5] and hybrid MoS_2 and silicon APD reported in [4]. In Ref. [4] the gain is calculated relative to current under zero bias, which explains the very high gain value. BP has smaller bandgap compared to InSe and MoS_2 which permits avalanche multiplication at low biases and promises high potential for telecom communication applications.

* The EQE and IQE are presented in absolute values.
** These were calculated from data reported in Ref. [4]